

# Self-Diffusion in Solutions of Polystyrene in Tetrahydrofuran: Comparison of Concentration Dependences of the Diffusion Coefficients of Polymer, Solvent, and a Ternary Probe Component

Ernst D. von Meerwall

Department of Physics, University of Akron, Akron, Ohio 44325

Eric J. Amis and John D. Ferry\*

Department of Chemistry, University of Wisconsin, Madison, Wisconsin 53706.

Received June 6, 1984

**ABSTRACT:** Pulsed field gradient spin-echo NMR has been used to measure the self-diffusion coefficients  $D$  at 30.0 °C of all three components of solutions containing polystyrene (PS), tetrahydrofuran (THF) as solvent, and hexafluorobenzene (HFB) as a probe molecule at low concentration. The polymer molecular weights ( $M$ ) ranged from 10 000 to 1 050 000 and concentrations ( $c$ ) from 0.0063 to 0.712 g/mL, from below the overlap concentration  $c^*$  to above the entanglement onset concentration  $c_e$ . The diffusion coefficients  $D_{\text{HFB}}$  and  $D_{\text{THF}}$  were independent of polymer molecular weight, and their dependences on polymer concentration were identical;  $D_{\text{HFB}}/D_{\text{THF}} \approx 0.74$ . The HFB friction coefficient  $\zeta_1 = kT/D_{\text{HFB}}$  was only slightly higher than the infinite dilution extrapolation value  $\zeta_{10}$  for  $c < 0.1$  but was higher by a factor of 550 at the highest concentration; its concentration dependence could be described by the free volume theories of Fujita and others. Values of  $D_{\text{PS}}$  covered a range of 5 logarithmic decades. A logarithmic plot of  $D_{\text{PS}}M^2$  (following certain scaling theories) against  $c$  did not give a single composite curve and showed no significant regions with slopes of  $-1.75$  or  $-3$  which are predicted by those theories. The effect of local friction could be taken into account, together with different behavior above and below  $c_e$ , as follows. For  $c^* < c < c_e$ ,  $D_{\text{PS}}M\zeta_1/\zeta_{10}$  was plotted logarithmically against  $c$ ; for  $c \geq c_e$ , the ordinate was  $\log(D_{\text{PS}}M^2\zeta_1/\zeta_{10})$ . The slopes were close to  $-1.75$  in both cases. Thus the scaling law predictions for entangled solutions, based on motion by reptation, appear to be correct if the dependence of local friction on free volume is taken into account. For unentangled solutions, the molecular weight dependence corresponds to the Rouse theory prediction for a free-draining macromolecule but the concentration dependence shows that there is substantial hydrodynamic interaction in the range  $c^* < c < c_e$ . The effective monomeric friction coefficient  $\zeta_{0E} = kT/PD_{\text{PS}}$ , where  $P$  is the degree of polymerization, depends on concentration quite differently from  $\zeta_1$  and at lower concentrations has unreasonably small values. The results are discussed in terms of a modification of the blob theory.

## Introduction

Studies of self-diffusion in polymer solutions have recently evoked much interest because of the information they provide on molecular dynamics in different concentration regimes, including tests of the dependence of the diffusion coefficient on concentration and molecular weight as predicted by current theories. The subject has been reviewed recently by Tirrell.<sup>1</sup>

Pulsed gradient spin-echo NMR measurements provide a powerful technique for studying the self-diffusion of both polymer and solvent in polymer solutions over wide ranges of concentration and molecular weight, as well as the diffusion of a ternary component such as another small molecule with a different nucleus whose motion can be followed independently, to compare its frictional resistance to translatory motion with those of the other components.<sup>2</sup>

Theoretical treatments of the concentration and molecular weight dependence of polymer self-diffusion,<sup>3</sup> as well as analysis of experimental data,<sup>4-6</sup> have often ignored the role of local segmental frictional resistance, although it has been taken into account in several investigations,<sup>7-11</sup> where it has been analyzed in terms of fractional free volume, following the formulations of Fujita<sup>12,13</sup> or Vrentas and Duda.<sup>14</sup> For this purpose, the simultaneous determination of self-diffusion coefficients for both polymer and small molecules is especially useful in order to compare the frictional resistance to translatory motion for the latter with that per monomer unit of the polymer. In *undiluted* polymer, when a series of different polymers is compared, the friction coefficient of a small molecule present in trace amounts ( $\zeta_1$ ) appears to be proportional to and similar in magnitude to the friction coefficient per monomer unit of the polymer ( $\zeta_0$ ) as derived from viscoelastic measurements in the transition zone by a free-draining Rouse model.<sup>15</sup> It has often been assumed that the same proportionality

of  $\zeta_0$  to  $\zeta_1$  would hold in concentrated solutions. In one example<sup>16</sup> (the system polyisobutylene-hexadecane), their concentration dependences were observed to be closely similar over the range of polymer weight fraction ( $w_2$ ) from 0.8 to 1.0.

The concentration dependence of  $\zeta_1$  or  $\zeta_0$  has been successfully described by free volume analysis in several specific cases. These include  $\zeta_1$  for hexadecane in polyisobutylene<sup>16</sup> in the range  $w_2 = 0.3$  to 1.0, paraffins in polyisoprene<sup>7,17</sup> from 0.5 to 1.0, and 1,3-dimethyladamantane in polybutadiene<sup>9</sup> from 0 to 1.0; also,  $\zeta_0$  from viscoelastic measurements in the system poly(vinyl acetate)-diethyl phthalate<sup>13</sup> for  $w_2 = 0.5$  to 1.0. These results have been taken as additional evidence for close similarity between  $\zeta_1$  and  $\zeta_0$ . However, a more direct comparison of frictional resistances should be provided by self-diffusion data on both components.

The self-diffusion coefficient of the polymer in a concentrated solution,  $D_2$ , determines the total friction coefficient of the molecule as  $\zeta_P = kT/D_2$ . To obtain the friction coefficient per monomer unit, the simplest calculation would be

$$\zeta_0 = \zeta_P/P \quad (1)$$

where  $P$  is the degree of polymerization; this assumes that the translatory motion of the macromolecule is free draining and uninfluenced by entanglements. It might be expected that this would be the case in a concentration range  $c^* < c < c_e$ , where  $c$  is g of polymer per mL of solution and the characteristic values are defined as follows:<sup>3,13</sup>

$$c^* = M/N_A R_G^3 \quad (2)$$

$$c_e = \rho M_e^0/M \quad (3)$$

where  $M$  is the molecular weight,  $N_A$  is Avogadro's number,

Table I  
Characterization of Polymers

| polymer | mol wt    | $M_w/M_n$ | $c^*$  | $c_e$ |
|---------|-----------|-----------|--------|-------|
| 1477    | 10 000    | <1.2      | 0.344  |       |
| 1478    | 37 400    | 1.04      | 0.120  | 0.508 |
| 705     | 179 000   | 1.07      | 0.034  | 0.106 |
| PC 5a   | 498 000   | 1.2       | 0.015  | 0.038 |
| 1479    | 1 050 000 | 1.1       | 0.0083 | 0.018 |

$R_G$  is the radius of gyration,  $\rho$  is the polymer density, and  $M_e^0$  is the average molecular weight between entanglements in the undiluted polymer. However, it appears from the present investigation that eq 1 gives values of  $\zeta_0$  of unrealistic magnitude whose concentration dependence is quite different from that of  $\zeta_1$ .

Solutions of polystyrene in tetrahydrofuran, chosen for this work, are of particular interest because of the availability of polymer samples with narrow molecular weight distribution and the existence of extensive data on this system from other recent investigations by entirely different experimental methods: forced Rayleigh scattering,<sup>6</sup> which also determines the diffusion coefficient of a polymer tagged with a chromophore, as well as that of a ternary small molecule with suitable optical absorption;<sup>11</sup> and dynamic light scattering,<sup>18</sup> in which the slow relaxation mode appears to be related to center of mass translational diffusion of the polymer.

In the present experiments, five polystyrenes ranging in molecular weight from  $1 \times 10^4$  to  $105 \times 10^4$  have been studied in solution in tetrahydrofuran at concentrations from 0.006 to 0.71 g/mL, together with approximately 6% hexafluorobenzene as a ternary component. In most solutions, the self-diffusion coefficients of all three components were determined. The ranges of concentration and molecular weight encompassed concentrations from below  $c^*$  to above  $c_e$ .

## Materials and Methods

**Sample Preparation.** All solutions for these experiments were prepared gravimetrically, from spectroscopic grade tetrahydrofuran THF (Aldrich), sharp molecular weight samples of linear polystyrenes, and 99% hexafluorobenzene HFB (Aldrich), weighed directly into 7-mm-o.d. NMR tubes. Five polystyrenes (four NBS reference polymers and one (PC5a) from Pressure Chemical) were used to cover 2 decades of molecular weight as shown in Table I. Also shown is the polydispersity index  $M_w/M_n$ , the overlap concentration  $c^*$  (calculated from eq 2 with  $R_G$  taken<sup>19,20</sup> as  $1.45 \times 10^{-9} M^{0.595}$  cm), and the entanglement onset concentration  $c_e$  (calculated from eq 3 with  $\rho = 1.05$  g cm<sup>-3</sup> and  $M_e^0 = 18 100$ ; the use of  $M_e^0$  instead of  $M_c^0$ , the critical molecular weight for the influence of entanglements on viscosity, is somewhat arbitrary.)<sup>21</sup> In any case, both  $c^*$  and  $c_e$  provide only a rough indication of the ranges of chain interactions. Approximately 6% of HFB was included in each solution. The polymer concentration  $c$  was calculated for each solution assuming volume additivity for the three components with the densities of THF and HFB taken as 0.889 and 1.618 respectively, at 30 °C. Cells were sealed under vacuum immediately after preparation with special care to prevent contamination by water. Samples were allowed to dissolve at 35 °C for at least 1 week with occasional gentle agitation before any NMR measurements were performed. All samples were clear, single phase, and homogeneous, and showed no evidence of convection or flow during the diffusion measurements. Measurements of several samples were repeated after 6 months of storage in the dark with no significant changes in the measured relaxation rates or diffusion parameters.

**Diffusion Measurements and Data Interpretation.** The pulsed gradient spin-echo (PGSE) method<sup>22,23</sup> of measuring self-diffusion was employed to study the Brownian motion of the three species of molecules. Our NMR/PGSE equipment and calibration,<sup>8,24</sup> data collection,<sup>25</sup> and data reduction methods<sup>26,27</sup> were used essentially as described, with various refinements. The pulsed NMR spectrometer operating at 33 MHz detected <sup>1</sup>H NMR

Table II  
Self-Diffusion Coefficients

| mol wt    | concn, g mL <sup>-1</sup> | log $D_{THF}$ , cm <sup>2</sup> s <sup>-1</sup> | log $D_{HFB}$ , cm <sup>2</sup> s <sup>-1</sup> | log $D_{PS}$ , cm <sup>2</sup> s <sup>-1</sup> |
|-----------|---------------------------|---|---|--|
| 10 000    | 0.383                     | -5.15   | -5.27   | -7.25  |
|           | 0.435                     | -5.40   | -5.55   | -7.87  |
|           | 0.496                     | -5.68   | -5.90   | -8.31  |
|           | 0.543                     | -5.73   | -5.90   | -8.50  |
|           | 0.628                     | -6.19   | -6.59   |  |
|           | 0.712                     | -7.04   | -7.34   |  |
| 37 400    | 0.176                     | -4.71   | -4.71   | -7.01  |
|           | 0.226                     | -4.82   | -4.94   | -7.32  |
|           | 0.266                     | -4.92   | -5.06   | -7.60  |
|           | 0.352                     | -5.11   | -5.25   | -8.03  |
|           | 0.475                     | -5.70   | -5.87   |  |
|           | 0.567                     | -5.98   | -6.21   |  |
| 179 000   | 0.0205                    | -4.49   | -4.62   | -6.81  |
|           | 0.0487                    | -4.52   | -4.65   | -7.01  |
|           | 0.0848                    | -4.60   | -4.71   | -7.42  |
|           | 0.128                     | -4.62   | -4.77   | -7.75  |
|           | 0.201                     | -4.86   | -4.87   | -8.28  |
|           | 0.313                     | -5.02   | -5.08   | -8.95  |
| 498 000   | 0.427                     | -5.50   | -5.59   |  |
|           | 0.0103                    | -4.43   | -4.58   | -7.19  |
|           | 0.0232                    | -4.48   | -4.61   | -7.37  |
|           | 0.0414                    | -4.50   | -4.64   | -7.57  |
|           | 0.0739                    | -4.56   | -4.695  | -8.12  |
|           | 0.138                     | -4.68   | -4.80   | -8.70  |
| 1 050 000 | 0.260                     | -4.98   | -5.03   | -9.38  |
|           | 0.0063                    | -4.46   | -4.60   | -7.39  |
|           | 0.0114                    | -4.46   | -4.59   | -7.53  |
|           | 0.0262                    | -4.50   | -4.62   | -7.80  |
|           | 0.0413                    | -4.52   | -4.65   | -8.35  |
|           | 0.0778                    | -4.67   | -4.69   | -8.93  |
|           | 0.164                     | -4.82   | -4.88   | -9.61  |

(polystyrene and THF) and <sup>19</sup>F NMR (hexafluorobenzene); all PGSE work was conducted at  $30 \pm 0.3$  °C.

Magnetic field gradient pulses of magnitude  $G$  from 100 to 300 G/cm and durations  $\delta$  up to 15 ms were separated by a delay  $\Delta$  of typically 10–80 ms; the radio-frequency pulse spacing was usually 25 or 50 ms. Digital signal averaging<sup>25</sup> was used to collect data of spin-echo height  $A$  vs.  $\delta$  at fixed  $G$  and  $\Delta$ . Diffusion coefficients  $D$  were obtained by least-squares techniques<sup>26,27</sup> from the slopes of semilog plots of  $A$  vs.  $\delta^2 G^2 (\Delta - \delta/3)$  with a correction term<sup>22–24</sup> for the presence of a small gradient  $G_0$  of 0.9 G/cm.

Since most of the diffusional echo attenuation was due to  $G$  rather than  $G_0$ , the effective time scale  $t = \Delta - \delta/3$  was well-defined<sup>22</sup> and nearly constant over each experiment. Attempts were made to detect non-Fickian diffusion by measuring  $D$  as function of diffusion time. In the present case it is easily shown that the coil dimensions of the polystyrenes in solution are smaller than the diffusion distance  $(2tD)^{0.5}$ , so that bounded segmental motions about the centers of mass of the macromolecules cannot dominate<sup>28</sup> the measured polystyrene diffusion coefficient,  $D_{PS}$ . Thus any non-Fickian diffusivity would indicate a spatially dependent coupling of self-diffusion to cooperative motions<sup>29</sup> which may involve many molecules<sup>30,31</sup> or voids.<sup>31</sup>

While it was possible to determine that the diffusivities of THF and HFB were independent of time between 10 and 150 ms, the crucial polystyrene diffusivities presented experimental problems because of the presence of the strong THF echo. It dominated even at the highest polymer concentrations because of its much longer spin-spin relaxation time  $T_2$ (THF). Thus, where extraction of  $D_{PS}$  was possible at all (see Table II), it is associated with a diffusion time in the range  $15 < t < 50$  ms.

As expected, the echo attenuation plots revealed single diffusion rates for both THF and HFB. The polydispersities of our polystyrenes were small enough that no modeling<sup>32</sup> with a range of diffusivities was attempted, particularly in view of the presence of the THF echo. Resolution of the proton echo into a strong, rapidly attenuated component (THF) and a much weaker, less easily attenuated part (PS) was performed via a nonlinear fit<sup>27</sup> of the sum of two individual attenuation patterns; the adjustable

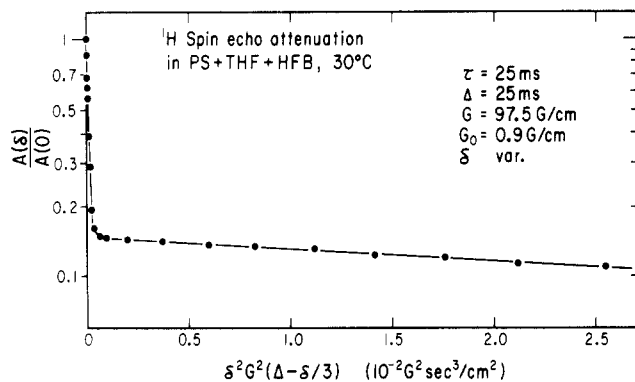


**Figure 1.** Proton spin-echo attenuation in solution with  $M = 176\,000$ ,  $c = 0.128$  g/mL. Abscissa contains correction term (not indicated) for presence of steady gradient  $G_0 = 0.9$  G/cm. Only lowest 40% of abscissa domain is shown; experimental error is approximately equal to symbol size. Solid line shows double-exponential fit to data; diffusivity of PS (final slope) is lower than that of THF by 3 orders of magnitude (see Table II).

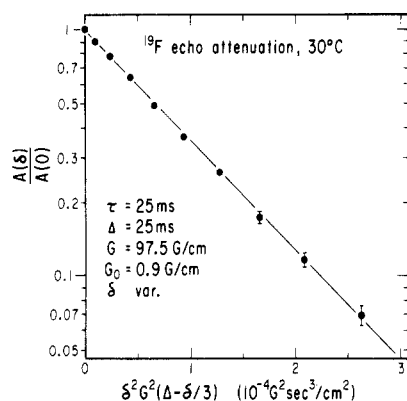


**Figure 2.** Fluorine spin-echo attenuation in same solution as for Figure 1. Abscissa is corrected for steady gradient  $G_0$ . Fitted solid line indicates single (HFB) diffusion route, approximately equal to that of THF.

parameters were  $D_{PS}$ ,  $D_{THF}$ , and the fraction of the unattenuated echo arising from THF. In cases where the PS echo was particularly small, this fit was relatively insensitive to its rate of attenuation. In such cases, improved values for  $D_{PS}$  were obtained by fitting a single-diffusivity model to only the final slope<sup>26,33</sup> of the echo attenuation data. It was possible to obtain resolvable proton echo attenuations when the polystyrene echo was as small as 2% of that of the THF, and when the two diffusivities differed by up to 4.5 orders of magnitude. Figures 1 and 2 show some typical attenuation data for  $^1\text{H}$  and  $^{19}\text{F}$ , respectively, with the optimally adjusted models.

## Results

Values of the self-diffusion coefficients of the tetrahydrofuran solvent, hexafluorobenzene probe, and the various polystyrenes are given in Table II for all polymer molecular weights and polymer concentrations. They cover a range of more than 5 decades; the lowest  $D_{PS}$  are near the lower limit of the PGSE technique. The presence of the strong THF echo noted above and the unfavorable ratio  $T_2(\text{PS})/T_2(\text{TMF}) \ll 1$  are the reasons for several missing  $D_{PS}$  entries for very concentrated solutions of polymers with low molecular weights. Experimental uncertainties for  $D_{THF}$  and  $D_{HFB}$  are approximately 5% while for  $D_{PS}$  they are 10%; reproducibility was considerably better.

The diffusion coefficients for the two small molecules THF and HFB are plotted logarithmically against polystyrene concentration in Figure 3. As expected,  $D_{THF}$  and  $D_{HFB}$  are independent of polymer molecular weight and

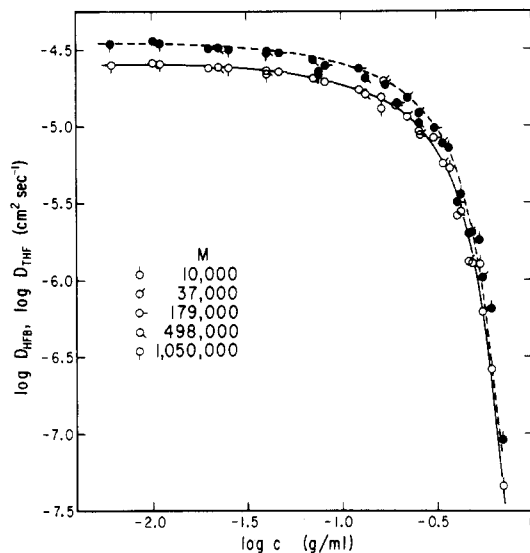


**Figure 3.** Self-diffusion coefficients of HFB (open circles) and THF (black circles) plotted logarithmically against polymer concentration. Polymer molecular weights are shown. Curves have identical shapes, displaced vertically by 0.13.

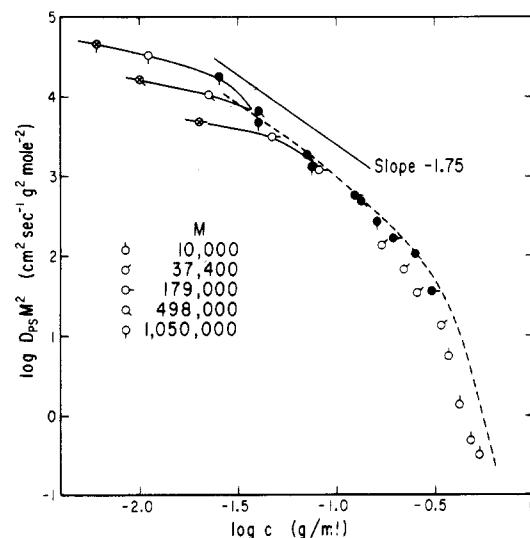


**Figure 4.** Self-diffusion coefficient of polystyrene multiplied by  $M^2$ , plotted logarithmically against polymer concentration. Molecular weights as shown. Crossed circles,  $c < c^*$ ; open circles,  $c^* < c < c_e$ ; black circles,  $c > c_e$ . Dashed curve: data of Wesson et al.<sup>6</sup> from forced Rayleigh scattering.

they have identical concentration dependence over two decades. This is shown by the smooth curve through the  $D_{HFB}$  points which is shifted vertically and drawn with dashes in agreement with the  $D_{THF}$  data. The vertical shift of 0.13, consistent with the relative sizes of THF and HFB, corresponds nearly to the cube root of their molecular weight ratio.

To present the polymer diffusion data,  $D_{PS}$  is multiplied by  $M^2$  to reflect a molecular weight dependence that is predicted by reptation theory<sup>4,19</sup> for entangled solutions ( $c > c_e$ ) and has been reported<sup>4,6</sup> both in this concentration range and in the lower range  $c^* < c < c_e$ . In Figure 4,  $D_{PS}M^2$  is plotted logarithmically against concentration. Data points in different concentration regimes are distinguished by crossed circles for  $c < c^*$  (dilute), open circles for  $c^* < c < c_e$  (semidilute but not entangled), and filled circles  $c > c_e$  (entangled). The dashed curve shows the substantial agreement with the results of Wesson et al.<sup>6</sup> for dye-labeled polystyrene (molecular weight range 32 000–360 000) in THF by the transient grating method

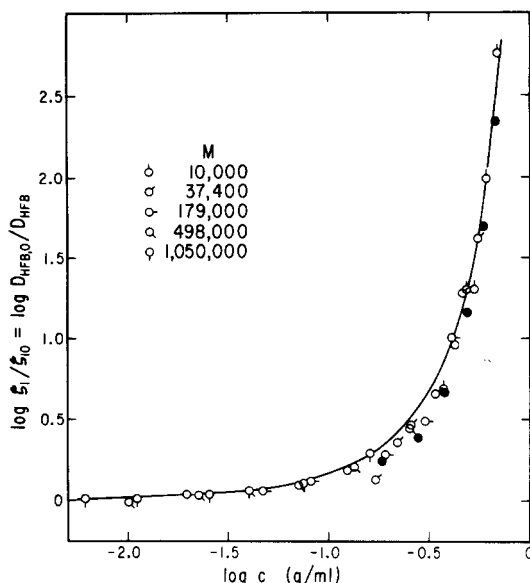


**Figure 5.** Ratio of diffusion coefficient of HFB extrapolated to zero polymer concentration to that at finite concentration, plotted logarithmically against  $c$ . Polymer molecular weights as shown. Black circles, data from methyl red self-diffusion in this system from forced Rayleigh scattering.<sup>11</sup> Solid curve calculated from free volume relation, eq 6.

of forced Rayleigh scattering. This agreement of results from two entirely different physical measurements is quite reassuring. According to the reptation model and scaling argument for self-diffusion<sup>19,29</sup> this plot should yield a universal curve with slope  $-1.75$  (as shown by line). Results such as those shown in Figure 4 are typically interpreted<sup>4,6,18,34</sup> as support for the reptation mechanism, even for concentrations and molecular weights where there is no chain entanglement. It should be noted, however, that there appear to be significant differences between entangled (filled circles) and unentangled (open circles) solutions, and the  $M^{-2}$  dependence is not convincing. It fails of course at concentrations below  $c^*$ , where data at different molecular weights diverge.

## Discussion

**Diffusion of THF and HFB.** In Figure 3,  $D_{\text{THF}}$  and  $D_{\text{HFB}}$  are insensitive to polymer concentration up to about  $c = 0.1$  but then drop rapidly with increasing concentration. We choose  $D_{\text{HFB}}$  for analysis since it is probably somewhat more precise. According to free volume theory in its simplest form,<sup>12</sup> the concentration dependence of either  $D_{\text{HFB}}$  or the friction coefficient  $\zeta_1 = kT/D_{\text{HFB}}$  is an exponential function of the fractional free volume  $f$ :

$$\zeta_1 = Ae^{B/f} \quad (4)$$

Comparison of  $\zeta_1$  to its value at a reference concentration,  $\zeta_{1r}$ , provides the following relation:<sup>13</sup>

$$\log (\zeta_1 / \zeta_{1r}) = (B/2.3)(1/f - 1/f_r) \quad (5)$$

and if the fractional free volumes are additive,<sup>35</sup> such that  $f = f_r + \beta'(v_1 - v_{1r})$ , taking  $B = 1$

$$\log (\zeta_1 / \zeta_{1r}) = \frac{-(v_1 - v_{1r})}{2.3f_r(f_r/\beta' + v_1 - v_{1r})} \quad (6)$$

where  $v_1$  and  $v_{1r}$  are the solvent (plus probe) volume fractions corresponding to  $\zeta_1$  and  $\zeta_{1r}$  and  $\beta'$  is a dimensionless parameter representing the excess fractional free volume contributed by the small molecules. The parameters  $f_r$  and  $\beta'$  are first chosen by selecting the highest

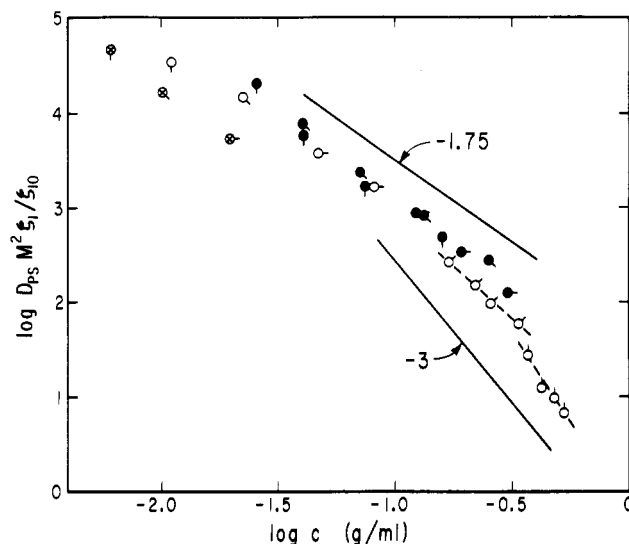


**Figure 6.** Logarithmic plot of  $D_{\text{PS}} M^2 / \zeta_1 / \zeta_{10}$  against polymer concentration. Key to concentration classification same as in Figure 4. Positions of solid lines are arbitrary.

polymer concentration for the arbitrary reference  $v_{1r}$ ; the results are  $v_{1r} = 0.339$ ,  $f_r = 0.106$ , and  $\beta' = 0.280$ . The latter two are reasonable values. For plotting, however, the curve is normalized to the limiting value of  $\zeta_1$  at zero polymer concentration (by extrapolation of Figure 3,  $\log \zeta_{10} = -2.605$ ), in Figure 5. The theoretical curve agrees with the data rather well over 2.8 logarithmic decades; again, the results are independent of polymer molecular weight. (Molecular weight dependence would be expected at lower molecular weights.<sup>8</sup>) Moreover, the friction coefficient ratios obtained from self-diffusion measurements of the dye methyl red by forced Rayleigh scattering<sup>11</sup> are included as filled circles. Again, the agreement between the two different experimental methods is remarkably good.

It may be remarked that the applicability of free volume theory in its simple form at very low concentrations is questionable. However, the concentration dependence here is so small that the test is not critical. The important feature is that the rapid increase in  $\zeta_1$  at higher concentrations can be explained by the difference in free volume (whereas the macroscopic viscosity, of course, increases far more rapidly than  $\zeta_1$  with concentration and also depends strongly on molecular weight).

**Diffusion of Polymer.** The slope at high concentrations in Figure 4 (also observed by many other workers<sup>4-6,11,18,30</sup>) is much steeper than that given by the power-law exponent of 3 which is the maximum predicted by scaling laws. Observation of the steep slope in Figures 3 and 5 suggests that the polymer diffusion is influenced by a concentration dependence of the local friction coefficient of the polymer similar to that of  $\zeta_1$ . The simplest attempt to remove the effect of free volume is to multiply  $D_{\text{PS}} M^2$  (from Figure 4) by the ratio  $\zeta_1 / \zeta_{10}$  for HFB from the data of Figure 5; the corresponding logarithmic plot is shown in Figure 6. The first success of this treatment is to reduce the sharp drop off of  $D_{\text{PS}}$  at high concentration, as found also by Nemoto, Yu, and co-workers.<sup>11</sup> From scaling law and reptation predictions,<sup>3,6,18,34</sup> the self-diffusion coefficient in a good solvent should be proportional to  $c^{-1.75}$  in semidilute solution. As the effective solvent quality decreases with higher polymer concentration the slope may go as far as  $c^{-3}$ , the  $\Theta$  prediction. Lines with slopes  $-1.75$  and  $-3$  are shown in Figure 6 and are plausible, as found also by Nemoto et al.<sup>11</sup> with a similar treatment. This indicates the importance of an increase in the local seg-

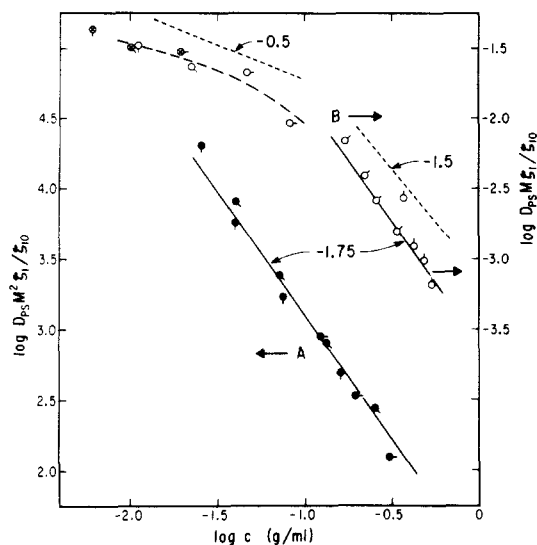


**Figure 7.** Logarithmic plots against concentration of  $D_{PS}M^2\zeta_1/\zeta_{10}$  for  $c > c_e$  (line A, at left) and  $D_{PS}M\zeta_1/\zeta_{10}$  for  $c < c_e$  (curve B, at right). Key to concentration classifications same as in Figure 4. Position of dashed lines are arbitrary.

mental frictional resistance which is not accounted for in scaling theories. A careful examination of Figure 6, however, reveals a disturbing feature, which is the inability of the  $M^2$  factor in the ordinate to produce a completely universal curve.

**Role of Entanglements.** At concentrations below or near the overlap concentration  $c^*$  it is expected, and has been observed,<sup>4,6,18,34</sup> that  $D_{PS}$  will no longer be proportional to  $M^{-2}$ . We observe this also. However, with very few exceptions,<sup>8</sup> it has been claimed that for high concentrations or undiluted polymer,  $D_{PS}$  is proportional to  $M^{-2}$  even for concentrations and/or molecular weights which cannot form entanglements ( $c$  or  $\rho$  less than  $c_e$ ). Actually, we have seen how the sharp drop in  $D_{PS}$  at high concentration in Figure 4 hides the failure of  $M^{-2}$  scaling; once those data are corrected for free volume changes as in figure 6, the low molecular weights, for  $c < c_e$ , are distinctly out of line. Similar effects on the apparent molecular weight exponents have been pointed out previously by von Meerwall<sup>8</sup> for diffusion studies and by Berry and Fox<sup>36</sup> for viscosity. It has been suggested<sup>4,6,18</sup> that the molecular weight dependence for  $D_{PS}$  in semidilute solution can be checked by plotting  $\log D_{PS}c^{1.75}$  vs.  $\log M$  or by measuring different molecular weights at fixed semidilute concentration. Neither of these methods is completely adequate since the first assumes that an unproven concentration scaling power will apply throughout the concentration/molecular weight range and the second requires the impossible situation that a wide range of molecular weights have overlapping scaling law windows. We use a different plot in Figure 7 where the  $D_{PS}$  data are separated into two sets: filled circles above the entanglement concentration  $c_e$  are plotted again as  $\log (D_{PS}M^2\zeta_1/\zeta_{10})$  (line A) and unfilled circles, below entanglement, are plotted with a single power of molecular weight,  $\log (D_{PS}M\zeta_1/\zeta_{10})$  (curve B); both are plotted against  $\log c$ . The  $M^{-1}$  dependence would be predicted by a Rouse model of hydrodynamically screened free-draining coils with no entanglement effects (i.e., no reptation).<sup>8</sup> This method of testing molecular weight exponents has some of the same ambiguities as the others but since we assume no concentration power law we have eliminated the influence of the changing effective solvent quality and this is a distinct advantage. Our conclusion from this analysis, taking account of the change in local friction, is that semidilute entangled solutions have

$M^{-2}$  dependence while unentangled solutions have  $M^{-1}$  dependence. The combination of local effective friction, ambiguous solvent quality, and the dual molecular weight dependences is the likely explanation for the peculiar molecular weight dependences which have been observed.<sup>5,18</sup>

The dashed curve in Figure 7 is drawn through the data at low concentration and has no theoretical significance except to show the  $M^{-1}$  scaling. The solid lines, however, are both drawn with  $-1.75$  slope which is the scaling prediction for good solvents. There is very good agreement with the data for the entangled solutions and unanticipated agreement with the data for unentangled solutions at higher concentrations. Given only the results for entangled solutions, two conclusions would appear: (1) reptation is the dominant diffusion mechanism ( $M^{-2}$ ) and (2) scaling theory with its concentration blobs moving in an effective local environment ( $\zeta_1/\zeta_{10}$  correction) describes the concentration dependence of diffusion ( $c^{-1.75}$ ). The second of these conclusions becomes questionable, however, when the unexpected  $c^{-1.75}$  region, which is derived by using the reptation hypothesis, is also observed for unentangled, nonreptating ( $M^{-1}$ ) solutions. We cannot say whether the observation is coincidental or indicative of a broader generality than is apparent from the scaling derivation. In the broadest sense, the essential feature which must be considered is the concentration dependence of hydrodynamic interaction.

**Hydrodynamic Screening.** As stated in the Introduction, previous comparisons the frictional resistances of small molecules and macromolecules have been based on calculation of a monomeric friction coefficient  $\zeta_0$  by eq 1, with the assumption that the motion of the polymer is free draining. Focusing attention on the data for  $c^* < c < c_e$  in Figure 7 (curve B at right), if the concentration dependences of  $\zeta_0$  and  $\zeta_1$  were identical, this curve should have zero slope. This can be seen since  $D_{PS} = kT/\zeta_p$  and according to eq 1 (since  $P = M/M_0$ , where  $M_0$  is the monomer weight) the right ordinate of Figure 7 is  $(kTM_0/\zeta_{10})(\zeta_1/\zeta_0)$ , which would be independent of concentration. If we use eq 1 to define an effective monomeric friction coefficient

$$\zeta_{0E} = \zeta_p/P \quad (7)$$

it is clear that  $\zeta_{0E}$  has an entirely different concentration dependence from that of  $\zeta_1$ , and presumably from that of the true monomeric friction coefficient of a free-draining molecule.

This can also be seen strikingly by comparing the concentration dependences of  $\zeta_1$  and  $\zeta_{0E}$  (unentangled solutions only) in Figure 8. At concentrations below about 0.3 g/mL,  $\zeta_{0E} < \zeta_1$ , and at  $c = 0.1$  it is smaller by about a factor of 4. Clearly the friction is much smaller than it would be for a free-draining molecule. But  $\zeta_{0E}$  increases with concentration much more rapidly than  $\zeta_1$  and becomes considerably larger than  $\zeta_1$  at high concentrations.

In scaling arguments, the reduction in friction in semidilute solutions is modeled as a change in size and number of "concentration blobs" within which frictional resistance is reduced by hydrodynamic interaction. In Figure 7, the slope of curve B at higher concentrations, instead of being zero, actually seems to approach the concentration power law of  $-1.75$  predicted by scaling arguments for semidilute solutions. This is unexpected because the latter are based in part on the reptation mechanism for diffusion, and reptation predicts  $D_s \propto M^{-2}$ , not  $M^{-1}$  as observed.

Another treatment of the semidilute/nonentangled solvent can be proposed recognizing that polymers in nonentangled solutions, lacking topological constraints, are free

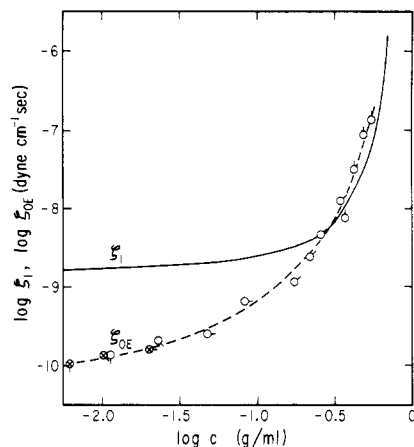


**Figure 8.** Comparison of  $\zeta_1$  for HFB (solid line, points omitted to avoid confusion) with  $\zeta_{0E}$  of polystyrene calculated from Rouse model, eq 7, for  $c < c_e$  only. Key to concentration classifications same as in Figure 4.

to diffuse by mechanisms other than reptation. At the same time, if the molecules overlap significantly ( $c > c^*$ ), there will be some screening of their hydrodynamic interaction perhaps as is described by scaling arguments. Consider the total frictional resistance of the polymer moving through the total solution which we previously described as

$$\zeta_p = P\zeta_{0E} \quad (8)$$

We can write this molecular friction in the framework of the "blob" theory<sup>34</sup> as the friction per blob  $6\pi\eta_e\xi_c$  times the number of blobs per chain  $P/P_c$

$$\zeta_p = P\zeta_{0E} = 6\pi\eta_e\xi_c P/P_c \quad (9)$$

Here  $P_c$  is the number of monomer units per blob,  $\eta_e$  is an effective local viscosity, and  $\xi_c$  is a measure of the blob radius. If the HFB molecule encounters the same  $\eta_e$ , its friction coefficient can similarly be written as

$$\zeta_1 = 6\pi\eta_e R_{HFB} \quad (10)$$

where  $R_{HFB}$  is its effective hydrodynamic radius. Combining eq 9 and 10 (and eliminating the undefined  $\eta_e$ ) gives an expression proportional to the quantity plotted on the right of Figure 7

$$\zeta_1/\zeta_0 = R_{HFB}P_c/\xi_c \quad (11)$$

According to scaling theory  $P_c \propto c^{-5/4}$ ,  $\xi \propto c^{-3/4}$  (good solvent);  $P_c \propto c^{-2}$ ,  $\xi \propto c^{-1}$  ( $\Theta$  solvent); and  $P_c \propto c^{-2}$ ,  $\xi_c \propto c^{-1/2}$  (marginal solvent,<sup>34</sup> intermediate between good and  $\Theta$  behavior). From these relations, one would predict the slope of curve B in Figure 7 to start at  $-0.5$  (good solvent) and to decrease to  $-1.5$  (marginal) or  $-1.0$  ( $\Theta$ ). Dashed lines of slope  $-0.5$  and  $-1.5$  are shown. These correspond plausibly to the data, and this treatment is the first step toward explaining concentration dependence of polymer diffusion in a range where topological restraints and reptation are absent but hydrodynamic interaction is screened to a varying extent.

**Relation to Viscoelastic Properties.** Two important quantities in linear viscoelasticity of concentrated polymer solutions can also be expressed in terms of a monomeric friction coefficient. According to the Rouse theory, which has often been applied to solutions in the range  $c^* < c < c_e$ , the solution viscosity  $\eta_0$  and terminal (longest) relaxation time  $\tau_1$  are given by

$$\eta_0 = \zeta_0 a^2 P N_A / 36 M_0 \quad (12)$$

$$\tau_1 = \zeta_0 a^2 P^2 / 6 \pi^2 k T \quad (13)$$

where  $a^2$  is the mean square end-to-end distance per monomer unit. Here the polymer molecules are assumed to be free draining. Combination of eq 1 and 12 shows that the product  $D_2\eta_0/c$  should be independent of concentration, as it was found to be for this system by Wesson et al.<sup>6</sup> Apparently  $\zeta_0$  in eq 12 should be replaced by  $\zeta_{0E}$  as it is in eq 7, i.e., a friction coefficient that is more strongly concentration dependent than that of a small molecule or a free-draining polymer.

In the same way, elimination of  $\zeta_0$  from eq 1 and 13 shows that the product of  $D_2\tau_1$  should be concentration independent. Does the concentration dependence of  $\tau_1$  resemble that of  $\zeta_1$  or that of  $\zeta_{0E}$  in Figure 8? In two cases, numerical values are available for polystyrene, though in different solvents. Measurements by Holmes<sup>37,38</sup> for  $M = 267\,000$ ,  $c = 0.02$ – $0.09$  in Aroclors show the strong concentration dependence and in fact  $\log D_{PS}\tau_1$  is approximately constant with  $D_{PS}$  taken from Table I for  $M = 179\,000$  (the effects of different solvent and somewhat different molecular weight presumably canceling out). Measurements by Martel et al.<sup>39</sup> for  $M = 400\,000$ ,  $c = 0.02$ – $0.09$  in Aroclor also show strong concentration dependence. Measurements by Adam and Delsanti<sup>40</sup> unfortunately do not provide data in an unentangled concentration range. Thus the effective monomeric friction coefficient controlling time scale of viscoelastic properties in semidilute solutions does not appear to be similar to  $\zeta_1$  for a small molecule, despite the useful correlation between these two quantities that has been observed in undiluted polymers.

## Conclusion

Evidently the diffusion of linear macromolecules in semidilute and concentrated solutions is influenced by four distinct, yet coupled, features: hydrodynamic interaction, effective solvent quality, topological constraints to isotropic chain motion, and free volume. While we have handled each of these effects in the present work, a more general approach, taking into account the coupling of the different influences, must be sought.

**Acknowledgment.** This work was supported in part by the Polymers Program of the National Science Foundation, Grants DMR-79-08299 and DMR-81-15462.

**Registry No.** PS (homopolymer), 9003-53-6; THF, 109-99-9; HFB, 392-56-3.

## References and Notes

- (1) Tirrell, M. *Rubber Chem. Technol.* **1984**, *57*, 523–556.
- (2) von Meerwall, E. D. *Adv. Polym. Sci.* **1983**, *54*, 1–29.
- (3) de Gennes, P.-G. *Macromolecules* **1976**, *9*, 587–593, 594–598.
- (4) Léger, L.; Hervet, E.; Rondelez, F. *Macromolecules* **1981**, *14*, 1732–1738.
- (5) Callaghan, P. T.; Pinder, D. N. *Macromolecules* **1981**, *14*, 1334–1340; **1984**, *17*, 431–437.
- (6) Wesson, J. A.; Noh, I.; Kitano, T.; Yu, H. *Macromolecules* **1984**, *17*, 782–792.
- (7) Ferguson, R. D.; von Meerwall, E. D. *J. Polym. Sci., Polym. Phys. Ed.* **1980**, *18*, 1285–1301.
- (8) von Meerwall, E. D.; Grigsby, J.; Tomich, D.; Van Antwerp, R. *J. Polym. Sci., Polym. Phys. Ed.* **1982**, *20*, 1037–1053.
- (9) von Meerwall, E. D.; Van Antwerp, R. *Macromolecules* **1982**, *15*, 1115–1119.
- (10) Fleischer, G. *Polym. Bull.* **1984**, *11*, 75–80.
- (11) Nemoto, N.; Landry, M. R.; Noh, I.; Kitano, T.; Wesson, J. A.; Yu, H. *Macromolecules* **1985**, *18*, 308–310.
- (12) Fujita, H. *Adv. Polym. Sci.* **1961**, *3*, 1–47.
- (13) Ferry, J. D. "Viscoelastic Properties of Polymers", 3rd ed.; Wiley: New York, 1980; pp 492–497.
- (14) Vrentas, J. S.; Duda, J. L. *J. Polym. Sci., Polym. Phys. Ed.* **1977**, *15*, 403–416, 417–439; **1979**, *17*, 1085–1096.
- (15) Chen, S. P.; Ferry, J. D. *Macromolecules* **1968**, *1*, 270–278.

- (16) Moore, R. S.; Ferry, J. D. *J. Phys. Chem.* **1962**, *66*, 2699-2704.
- (17) Vrentas, J. S.; Duda, J. L.; Ling, H. D. *J. Polym. Sci., Polym. Phys. Ed.* **1984**, *22*, 459-469.
- (18) Amis, E. J.; Han, C. C. *Polymer* **1982**, *23*, 1403-1406; *Polymer* **1984**, *25*, 650-658.
- (19) de Gennes, P.-G. "Scaling Concepts in Polymer Physics"; Cornell University Press: Ithaca, NY, 1979.
- (20) Decker, D. Thesis, Strasbourg, 1968.
- (21) Reference 13, pp 212, 243.
- (22) Tanner, J. E. Ph.D. Thesis, University of Wisconsin, 1966.
- (23) Stejskal, E. O.; Tanner, J. E. *J. Chem. Phys.* **1965**, *42*, 288-292.
- (24) von Meerwall, E.; Ferguson, R. D. *J. Appl. Polym. Sci.* **1979**, *23*, 877-885.
- (25) von Meerwall, E.; Burgan, R. D.; Ferguson, R. D. *J. Magn. Reson.* **1979**, *34*, 339-347.
- (26) von Meerwall, E. *Comput. Phys. Commun.* **1979**, *17*, 309-316.
- (27) von Meerwall, E.; Ferguson, R. D. *Comput. Phys. Commun.* **1981**, *21*, 421.
- (28) Cosgrove, T.; Warren, R. F. *Polymer* **1977**, *18*, 255-258.
- (29) de Gennes, P.-G. *J. Chem. Phys.* **1971**, *55*, 572-579; *J. Phys. (Orsay, Fr.)* **1975**, *36*, 1199-1203.
- (30) Callaghan, P. T.; Pinder, D. N. *Macromolecules* **1980**, *13*, 1085-1092.
- (31) Zupancic, I.; Lahajnar, G.; Blinc, R.; Reneker, D. H.; Vander-Hart, D. L. *J. Polym. Sci., Polym. Phys. Ed.*, in press.
- (32) von Meerwall, E. *J. Magn. Reson.* **1982**, *50*, 409-416.
- (33) von Meerwall, E.; Tomich, D.; Hadjichristidis, N.; Fetters, L. *J. Macromolecules* **1982**, *15*, 1157-1163.
- (34) Schaefer, D. W.; Han, C. C. In "Dynamic Light scattering and Velocimetry: Applications of Photon Correlation Spectroscopy"; Pecora, R., Ed.; Plenum Press: New York, 1982.
- (35) Fujita, H.; Kishimoto, A. *J. Chem. Phys.* **1961**, *34*, 393-398.
- (36) Berry, G. C.; Fox, T. G. *Adv. Polym. Sci.* **1968**, *5*, 261-357.
- (37) Holmes, L. A. Ph.D. Thesis, University of Wisconsin, 1967.
- (38) Ferry, J. D. "Viscoelastic Properties of Polymers," 2nd ed.; Wiley: New York, 1970; p 230.
- (39) Martel, C. J. T.; Lodge, T. P.; Dibbs, M. G.; Stokich, T. M.; Sammler, R. L.; Carriere, C. J.; Schrag, J. L. *Faraday Symp. Chem. Soc.* **1983**, *18*, 173-188.
- (40) Adam, M.; Delsanti, M. *J. Phys. (Orsay, Fr.)* **1983**, *44*, 1185-1193.

## Molecular Weight Scaling of the Transport Properties of Polyacrylamide in Water

Patricia M. Patterson and Alex M. Jamieson\*

Department of Macromolecular Science, Case Western Reserve University, Cleveland, Ohio 44106. Received November 14, 1983

**ABSTRACT:** Measurements of single-chain  $z$ -average translational diffusion coefficients,  $D_{t,z}^0$ , and radii of gyration,  $R_{g,z}$ , by photon correlation spectroscopy and intrinsic viscosities,  $[\eta]$ , of several polyacrylamide (PAAm) fractions in 0.1 M NaCl with 0.02 wt %  $\text{NaN}_3$  are reported. Intrinsic viscosity data are insensitive to NaCl concentration up to 0.5 M, suggesting that the chain expansion of PAAm is independent of ionic strength. Our results are compared with recent literature data in which a variety of anomalous excluded-volume exponents for these quantities have been reported. We find good agreement between our data for  $[\eta]$  and  $R_{g,z}$  with the earlier results but significant discrepancies when comparing our  $D_{t,z}^0$  results with the weight-average values,  $D_{t,w}^0$ , in the literature. The effect of polydispersity on the experimental data is discussed in terms of the Schulz-Zimm distribution. In agreement with our observations,  $z$ -average diffusion coefficients are expected to be numerically consistent with the intrinsic viscosity data and, to a lesser extent, with experimental measurements of  $R_{g,z}$ , provided the weight-average molecular weight  $\bar{M}_w$  is used as a scaling parameter. Substantial discrepancies in scaling exponents are liable to occur from the comparison of  $D_{t,w}^0$  against  $\bar{M}_w$  for polydisperse systems. Within experimental uncertainties our data  $D_{t,z}$  and  $[\eta]$  data for the PAAm-0.1 M NaCl system are consistent with typical literature data for flexible-chain molecules in good solvents.

### Introduction

Modern theories of chain statistics<sup>1</sup> lead to a variety of simple scaling laws for the molecular weight, temperature, and concentration dependence of the structural and dynamic properties of chain molecules in dilute<sup>2,3</sup> and semidilute solutions.<sup>4-6</sup> In the present paper, we are interested in the prediction of statistical theories for single-chain properties. The relevant experimental quantities are the radius of gyration,  $R_G$ , and the Stokes hydrodynamic radius,  $R_H$ , the latter being derived from the limiting translational diffusion coefficient,  $D_t^0$ , the limiting sedimentation coefficient,  $S^0$ , or the intrinsic viscosity,  $[\eta]$ . Scaling laws for these properties are expressed in terms of characteristic excluded-volume exponents:

$$R_G \sim N^{\nu_G} \quad (1)$$

$$R_H \sim N^{\nu_H} \quad (2)$$

and

$$[\eta] \sim N^a \quad (3)$$

For polymers in good solvents,  $\nu_G = 0.6$ , while, for  $\Theta$  solvents,  $\nu_G = 0.5$ . For marginal conditions,  $\nu_G$  may exhibit apparent values intermediate between 0.5 and 0.6, corre-

sponding to crossover from ideal statistics at short distances to excluded-volume contribution at large distances (higher molecular weight).

Experimentally, for polymers in the asymptotic regimes of good and  $\Theta$  conditions, the predicted behavior of  $\nu_G$  has been confirmed<sup>7</sup> in the molecular weight range  $250\,000 < \bar{M}_w < 10^6$ . On the other hand, flexible-chain molecules of comparable molecular weights in very good solvents<sup>8,9</sup> exhibit values of  $\nu_H \sim 0.56$ , rather than the anticipated value of 0.6. Similarly, the experimental Mark-Houwink exponent  $a$  is usually smaller than 0.8 for flexible coils in good solvents. Physically, these observations have been interpreted<sup>2,3</sup> to indicate that the crossover regime in chain statistics occurs more gradually in  $R_H$  and  $[\eta]$  than in  $R_G$ . Weill and des Cloizeaux<sup>3</sup> have proposed that the exponent  $a$  should be related to both  $\nu_G$  and  $\nu_H$ . Thus, they suggest

$$M[\eta] \sim R_G^2 R_H \quad (4)$$

and hence

$$1 + a = 2\nu_G + \nu_H \quad (5)$$

This result contrasts with the earlier expression of Flory and Fox<sup>10</sup>

$$M[\eta] \sim R_G^3 \quad (6)$$